Study of fatigue crack mechanism on an armco iron in the gigacycle fatigue by temperature recording and microstructural observations

Chong Wang, Danièle Wagner, Claude Bathias

Study of fatigue crack mechanism on an armco iron in the gigacycle fatigue by temperature recording and microstructural observations

Chong WANG[1], Danièle WAGNER[1*], Claude BATHIAS[1]

[1] University Paris Ouest Nanterre La Défense – LEME Laboratory – 50, rue de Sèvres – 92410 VILLE D'AVRAY – France

[*]Corresponding author : daniele.wagner@u-paris10.fr ,

Abstract: Whatever the fatigue domain, the fatigue crack mechanism consists of an initiation crack stage (stage I) and a propagation stage (stage II). For materials without inclusions with a single phase, the first damage events in the stage I are due to the occurrence of Slips Marks (SM) on the specimen surface.

In this study, the fatigue crack mechanism was studied in the VHCF domain on a body centered cubic Armco iron (with 80ppm of carbon content).The tests were performed on a piezoelectric fatigue machine on plate specimens. During the tests, the microstructure evolution was observed by optical microscope, and the temperature recording on the specimen surface was achieved by an infrared camera. After the failure specimen, fractographic observations were performed under a Scanning Electron Microscope;

From the temperature recording on the specimen surface near the section where the fracture occurs, the spatio temporal localization of the point where the temperature was the highest was achieved. The highest temperature corresponds to the crack tip where the plastic zone takes place. This allows to follow the evolution of the crack tip during the test. The results are compared with the fractographic examinations on the fracture surface, and the number of cycles in each stage can be calculated.

Keywords: Very High Cycle Fatigue, fatigue crack mechanism, Armco iron, piezoelectric device, Slips Marks, infrared thermography

1. Introduction

Whatever the fatigue domain, the fatigue crack mechanism consists of an initiation crack stage (stage I) and a propagation stage (stage II). For materials without inclusions with a single phase, the first damage events in the stage I are due to the occurrence of Slips Marks (SM) on the specimen surface [1,2]. At the beginning of the long crack propagation stage, striations occur (stage II).

Previously, the temperature recording was performed on the surface of cylindrical specimens [4,5] on materials with inclusions which leads to subsurface crack initiations with "fish eyes" formations .

In this paper, flat specimens were used in order to improve the temperature recording on the surface specimen. The studied material is an Armco iron without inclusions which leads to a surface crack

initiation. With a flat surface, the spatiotemporal localization of the point where the temperature was the highest was possible. The highest temperature corresponds to the crack tip during the test. Then, the results are compared with the fractographic examinations for identification with each stage.

2. Material

The studied material is a polycrystalline α iron whose chemical composition is given in Table1. The carbon content is 80ppm. The microstructure is ferrite with equiaxe grains. The ferrite grain size is included in 10 to 40 μm. No specifically orientation was observed by EBSD. Yield Stress is 240 MPa.

Table 1: Chemical composition of studied material

C	P	Si	Mn	S	Cr	Ni	Mo	Cu	Sn	Fe
0.008	0.007	0.005	0.048	0.003	0.015	0.014	0.009	0.001	0.002	Balance

3. Experimental procedure

3.1. Mechanical and Thermal Procedure

Tests were performed on a piezoelectric fatigue machine designed by C. Bathias and co-workers [6].
For the reason of surface observation condition by IR camera, a new design of 1 mm flat specimen (Fig. 1) was used to carry out fatigue tests. Specimen, special attachment and piezoelectric fatigue machine constituted the resonance system working at 20kHz. The cyclic loading is tension-compression . The stress ratio is then R_σ = -1. For this test, the applied stress amplitude $\Delta\sigma$ was 175 MPa, and the number of cycles to failure 3.2155×10^7 cycles

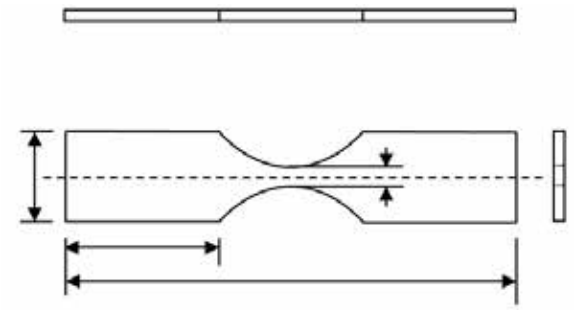

Fig. 1: Design of flat specimen

A CEDIP Orion infrared camera was used to record the temperature evolution during the test.The frequency of the camera was 50Hz and the aperture time was 100 μs.
Before testing, both side surface of the flat specimen were electrolytic polished. One side surface of the flat specimen was etched and another side painted in black color to have the surface emissivity close to 1.

4. Results

4.1. Thermal results

Figure 2 shows the entire temperature recording versus the number of cycles on the specimen surface during the test. As previously published [4], the temperature has a quick increase at the beginning of the test and tends progressively towards an asymptotic until the fatigue crack growth in mode II leading to the failure . Higher is the stress, higher is the temperature level.

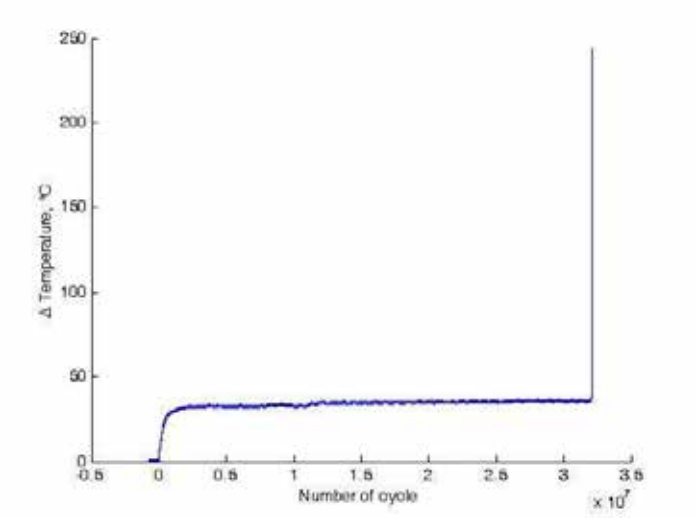

Figure 2: Temperature evolution versus number of cycles

From these data, the temperature profile (Figure 3) along the specimen width was extracted for the 168 latest pictures captured by the camera, that is to say from $3.2086.10^7$ cycles to $3.2153.10^7$ cycles (number of the cycles at the failure).

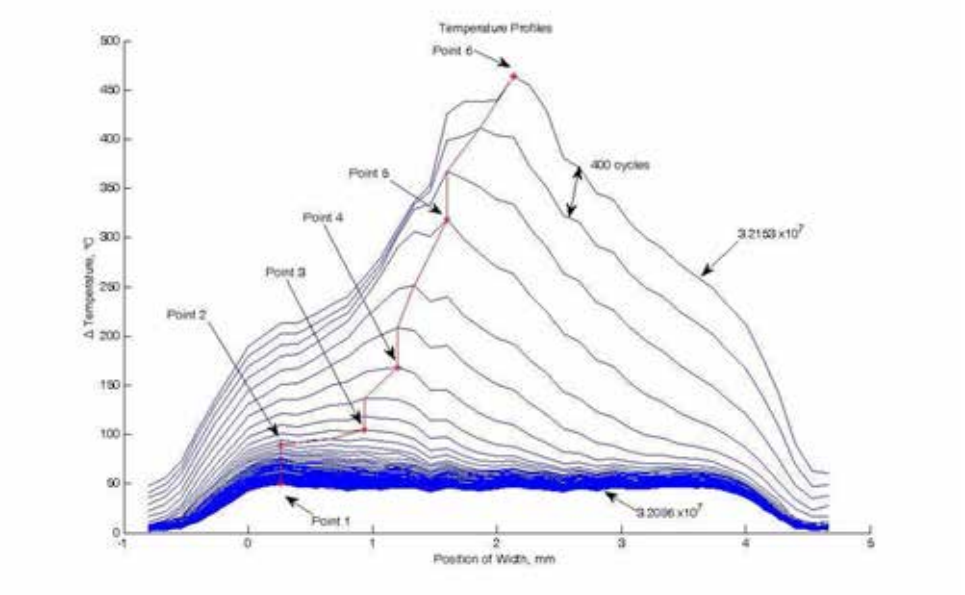

Figure 3 : Temperature profile along the specimen width

Between each profile, 400 cycles are performed. The red line on the figure 3 is the location where the temperature is maximum along the profile. Before $3.2086x10^7$ cycles, it was not possible to determine a location where the temperature was maximum along the profile. For this test, the crack initiation site appeared on the left side of the specimen (on the left side of the figure 3). The locations of the points 1/2,3,4,5,6 where the maximum temperature rapidly increases were determined. From the specimen corner, the locations of the different points are : points 1 et 2 at 267 µm, point 3 at 933 µm, point 4 at 1200 µm, point 5 at 1600 µm, point 6 at 2000µm. The corresponding numbers of cycles are : N_1 (point 1) at $3.2086 x10^7$ cycles, N_2 (point 2) at $3.2148x10^7$ cycles, N_3 (point 3) at $3.2149x10^7$ cycles, N_4 (point 4) at $3.2151x10^7$ cycles, N_5 (point 5) at $3.2152x10^7$ cycles, N_2 (point 2) at $3.2153x10^7$ cycles and the number of cycles at fracture N_f to $3.2155x10^7$ cycles.

During the end of this test, the maximum temperature location moves from the left to the right of the specimen width in agreement with the increase of the fatigue crack length and the increase of the plastic zone ahead the fatigue crack tip.

4.2. Fractographic results

The fracture surface and the polished specimen surface (where the temperature was recorded) were observed under Scanning Electron Microscope (Figure 4a and b). Until the point 5, the fracture surface is flat and correspond to the plane strain fatigue crack. Between the point 5 and 6, the fracture surface presents shear lips.

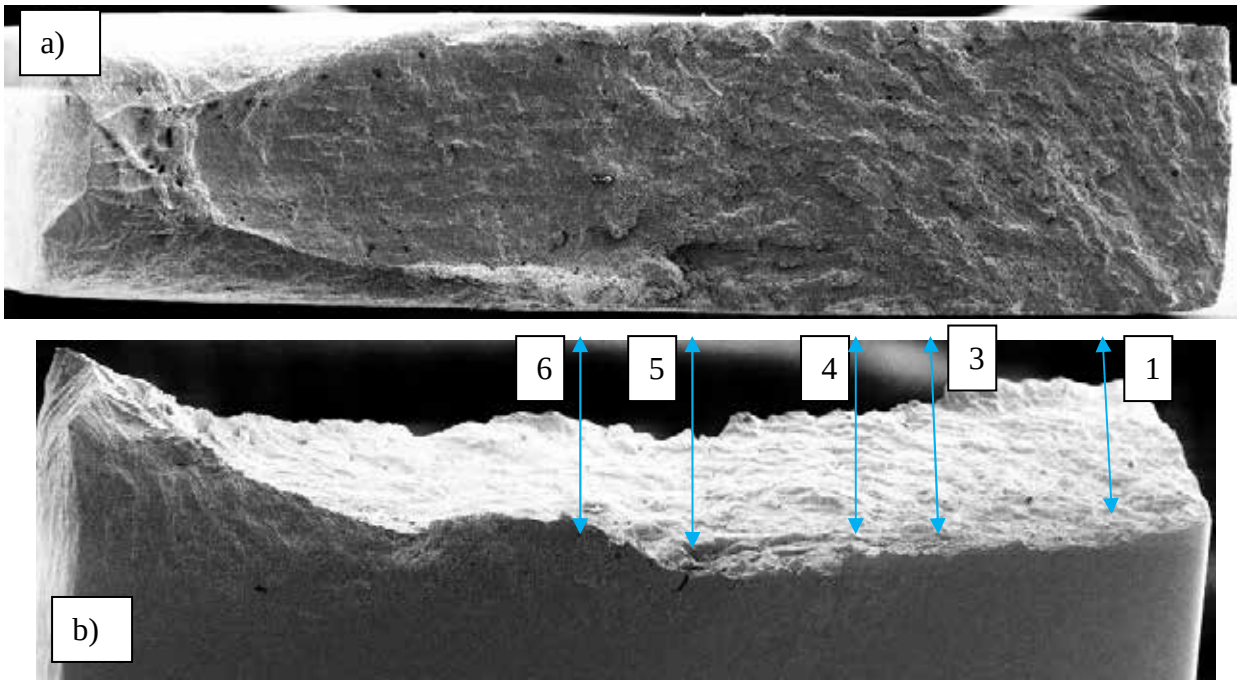

Figure 4a and b: SEM observations of the whole fracture and polished surface

The enlargement of the plane strain fatigue crack (Figure 5a) shows two main zones separated by the line at the point 3. The crack initiation site is located in the lower edge. In the stage I (Figure 5b), the trace of the grains in which Persistant Slips Bands (PSB) have appeared as previously shown [7] are visible. After the point 3, the stage II of long crack propagation begins with striations. At the beginning of this stage II, the striations are not well established (Figure 5c), whereas after the point 4 (and the corresponding line), the striations are well defined (Figure 5d).
The lower side of the specimen has been more particularly observed (Figure 6a,b,c). The figure 6c is the picture around the point 3 where a change in fracture surface can be observed. After the point 3, striations are present and correspond to the crack propagation as previously reported. Between the specimen corner and the point 3, another fracture surface change appears at the point 1. On the right side of the photo, the grain traces are clearly observed, whereas after the point 1 (Figure 6b), the fracture surface appearance change, change which is attributed to the transition from the crack initiation stage (stage I) to the short crack propagation.
From these observations, the locations of the different points can be measured. The results are: point 1 : ~ 294 μm, point 3 : ~ 882 μm, point 4 : ~ 1294 μm, point 4 : ~ 1629 μm.

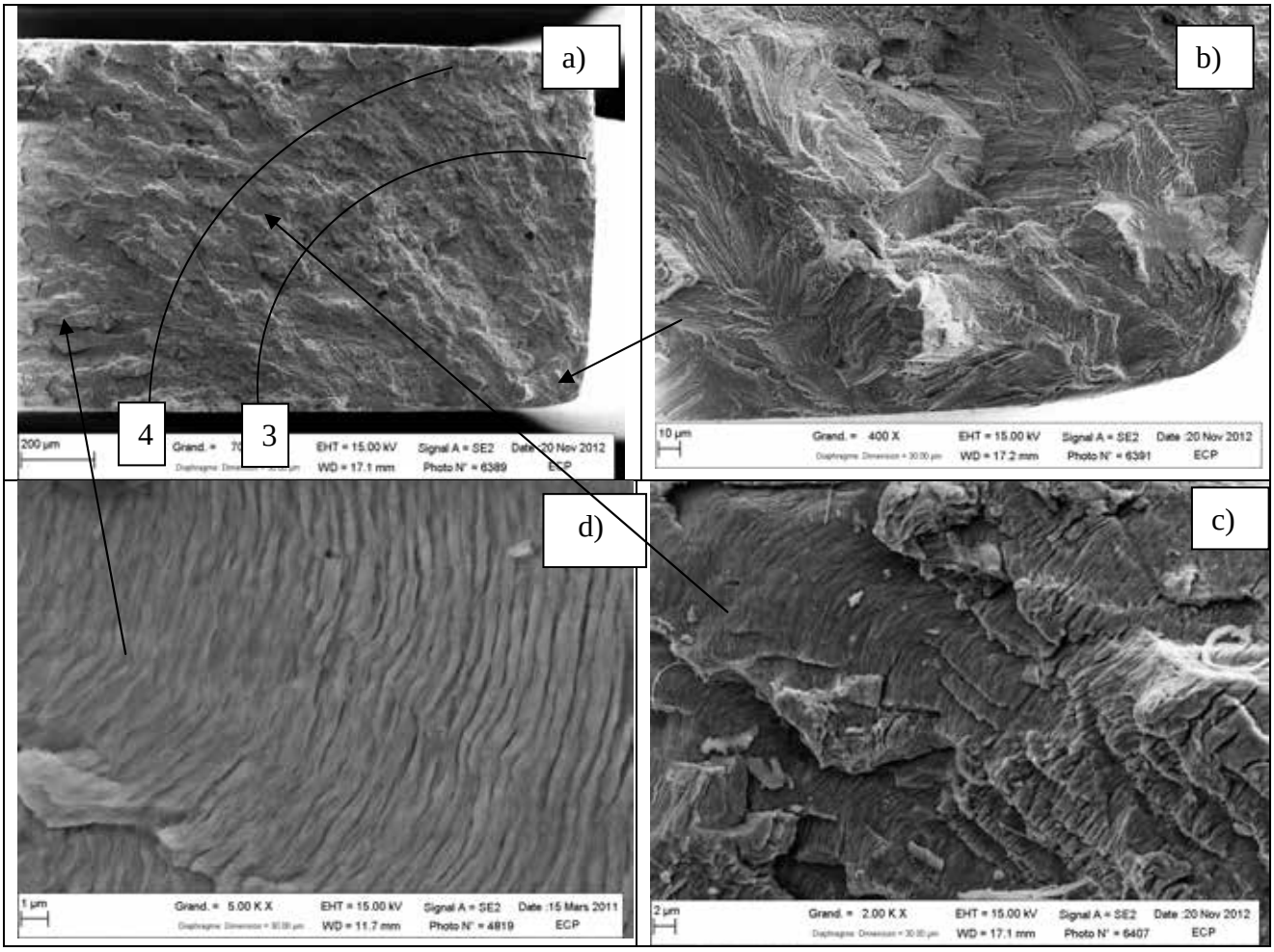

Figure 5 a)b)c)d) : SEM plane strain fatigue crack surface and details of each stage

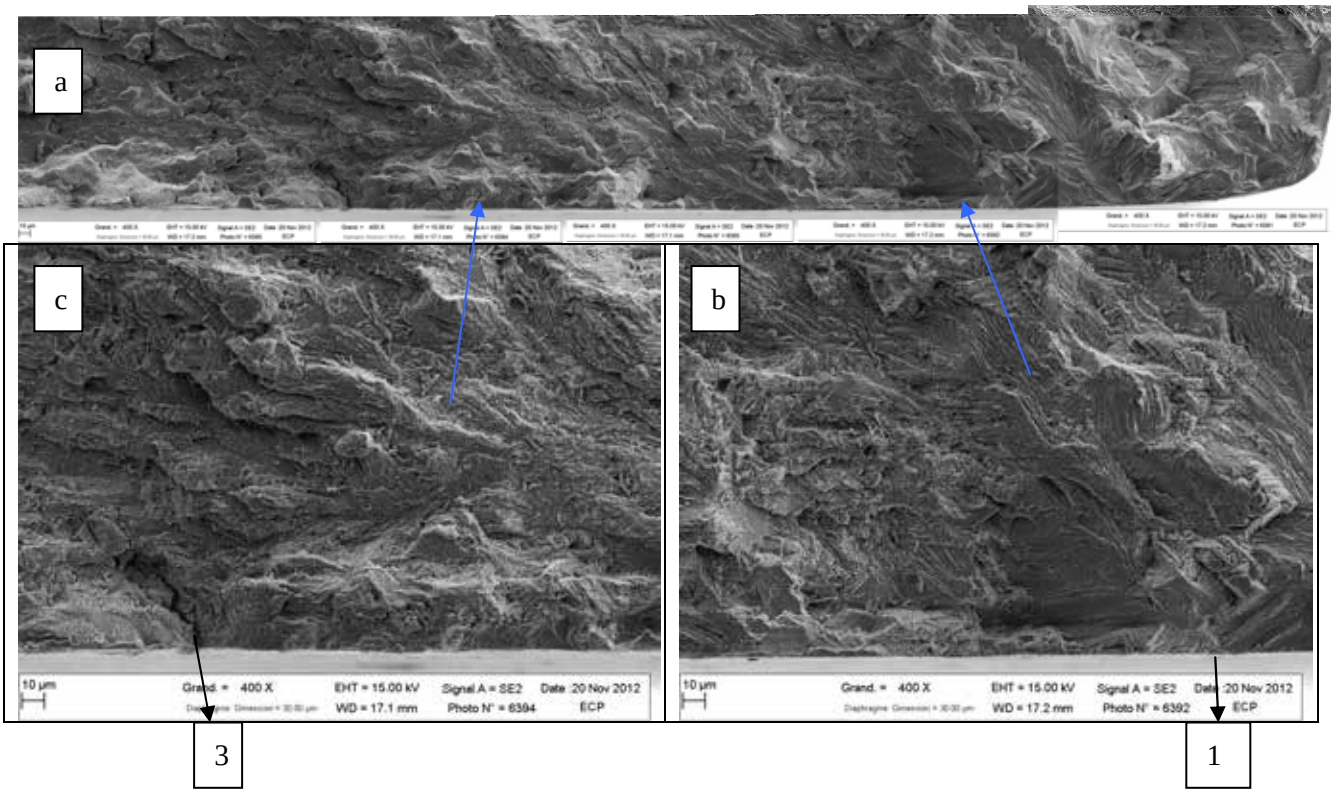

Figure 6 a)b)c: SEM observations of the fracture surface lower side (side where the temperature was achieved)

5. Discussion

The figure 7 a)b show the comparison between thermal results (yellow lines) and fracture surface observations. The agreement between the two data is very good.

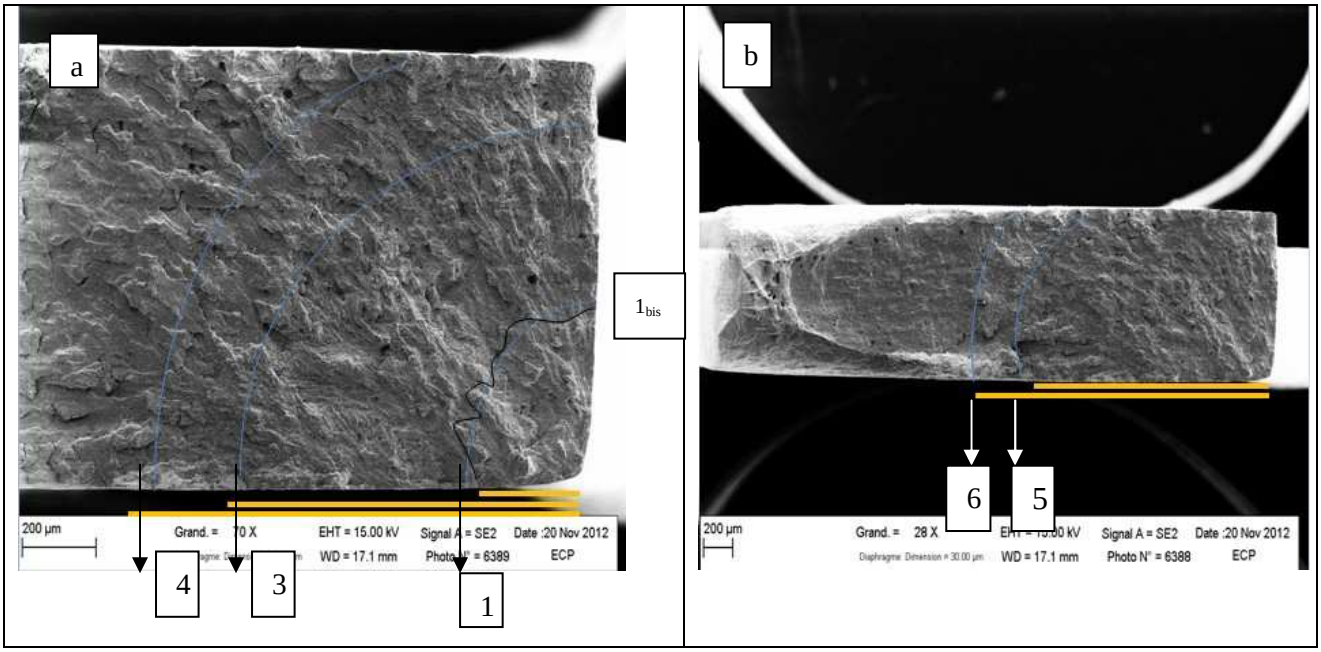

Figure 7a)b) :Comparison between thermal results (yellow lines) and fracture surface observations

(blue lines)

- When the number of cycles is below $3.2086x10^7$ cycles, the temperature is the same on the overall width of the specimen. The PSB formation on specimen surface are scarce and located on both side of the middle section of the specimen [7,8]. The intrinsic dissipation d_1 (specific heat source due to PSB) measured from the temperature measurement on the specimen surface is about 5°C/s [8]. There is no crack on the specimen surface.
- At the number of cycles $N = 3.2086x10^7$, the temperature profile on the specimen width shows a point (point 1, figure 3 and 7a) with a higher temperature. At this number of cycles, there is a rapid coalescence of PSB on specimen surface. Probably, the microcrack (due to the PSB) is also opened on the surface thickness of the specimen (point 1bis, figure 7a), and then, there is a coalescence between microcracks on the two surfaces (width and thickness). These points (1 and 1bis) correspond to the transition between crack initiation stage and short crack propagation stage (figure 6b).On the figure 7a, according to the all SEM observations (not presented here), this transition on the fracture surface has been reported. From the point 1, the temperature maximum increases, but this point does not move on the specimen width. This due to the formation of the crack initiation area between point 1 and 1bis When the crack spreads from point 1 to point 1bis, the ΔK threshold is reached. The calculation according to the blue line is 4.1 MPa$\sqrt{m}$, which correspond to a plastic zone size of ~ 47μm. The number of cycles $N = 3.2086x10^7$ is the number of cycles at the crack initiation N_i. This allows to calculate the ratio N_i/N_f equal to 0.9978. So, 99.8% of the total life is devoted to the initiation of the crack. As previously reported for the subsurface crack initiation in the gigacycle fatigue domain [4-5, 9-11], the major part of the total life is devoted to the crack initiation.
- Between point 1 / 1bis and 3, it is the fast short crack propagation. The length crack on the surface goes from 294 to 882 μm. At the point 3, the ΔK is 10.7 MPa$\sqrt{m}$, which correspond to a plastic zone size of ~317 μm, and the d_1 about 20°C/s [8].
- From the point 3, the long crack propagation begins, with the occurrence of striations. From this point (figure 8), the crack length and the temperature increase favors related to the high dislocation density the formation of many PSB in the plastic zone ahead the crack tip (figure 8).
- Then, the fatigue crack propagation goes on to the point 5. At this point, the d_1, reachs around 400°C/s (unpublished results).

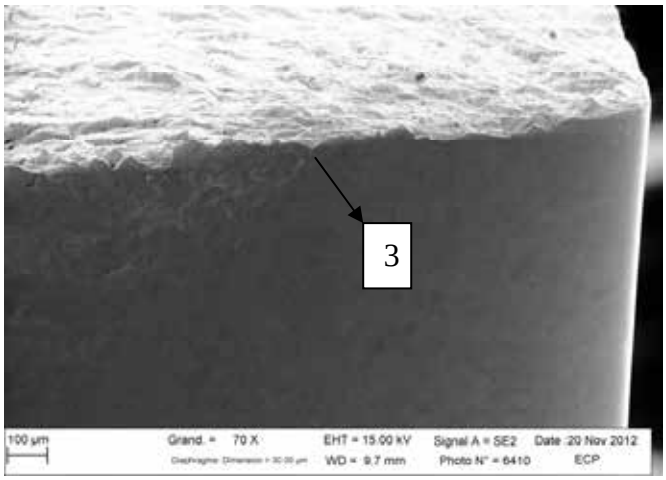

Figure 9: SEM observations of the high density PSB in the long crack propagation stage

From each point on the figure 3, the number of cycles can be calculated and reported on the curve

temperature versus number of cycles. Figure 9 is an enlargement of the end part of Figure 2, where the different points are reported. As previously published [5,9] for subsurface observations, the number of cycles of crack initiation N_i, corresponds to the weak temperature increase (point 1). The number of cycles between point 1 and 2 (Figure 9) corresponds to the crack initiation stage. Between point 2 and 3, the fast short crack propagation takes place. After the point 3, the plastic zone ahead the crack tip (figure 9) produces a great lot of PSB and then a great number of specific heat sources (PSB formation which are only visible on the specimen surface). The intrinsic dissipation d_1 and so the temperature grows rapidly until fracture.

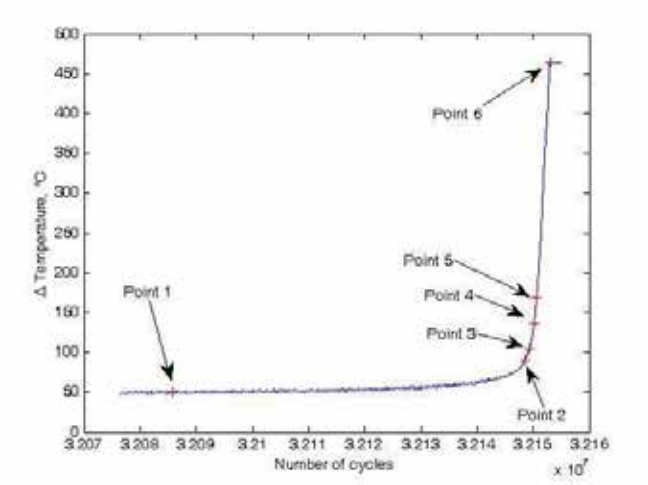

Figure 9: End of the temperature evolution versus number of cycles curve in relation with the number of cycles in each stage

6. Conclusion

In this paper, temperature follow-up on the surface of flat specimen for a ferrite Armco iron in the gigacycle fatigue domain is compared to the fracture surface observations made by SEM. The good agreement between thermal and SEM results allows to drawing the conclusions below:

- the crack initiation at the number of cycles N_i is due to a rapid coalescence of the PSB on the specimen surface (point 1 and 1bis). Then, the crack initiation spreads over the thickness of the specimen (coalescence of PSB between point 1 and 1bis in specimen volume) to achieve ΔK threshold (point 2) of about 4 MPa$\sqrt{m}$. In this test, more than 99% of the total life is devoted to the crack initiation.
- when the crack propagation (stage II) occurs, the temperature at the crack tip rapidly increases, firstly in short crack propagation regime (point 2→3), and then in a long crack propagation regime (point 3→5). In the long crack propagation regime, the number of PSB is very important, and so the specific heat sources and the temperature increase rapidly.

ACKNOWLEDGEMENTS

This research was supported by the grant from the project of Microplasticity and energy dissipation in very high cycle Fatigue (DISFAT, project No. ANR-09-BLAN-0025-09), which funded by the National Agency of Research, France (ANR). Aknowledgements are due to F. Garnier (Ecole Centrale de Paris) for the SEM observations.

REFERENCES

[1] S. Suresh, Fatigue of Materials, Cambridge University Press, Cambridge, UK, 2006
[2] C. Bathias, A. Pineau, Fatigue des matériaux et des Structures 1, Lavoisier, Paris, 2008
[3] H. Mughrabi, The Strength of Metals and Alloys, P. Haasen, V. Gerold, G. Kostorz, (Ed.), Pergamon Press, Oxford, 1980
[4] D. Wagner, N. Ranc, **C.** Bathias**,** P. Paris, Fatigue crack initiation detection by an infrared thermography method, Fat. Fract. Engng Mater Struct 33, (2009) 12-21
[5] N. Ranc, D**.**Wagner**,** P.C. Paris, Study of thermal effects associated with crack propagation during very high cycle fatigue, Acta Materiala **56,** (2008), 4012-4021
[6] C. Bathias, P. C. Paris, Gigacycle Fatigue in Mechanical Practice, Marcel Dekker, New York, 2004
[7] C. Wang, D. Wagner, Q.Y. Wang, C. Bathias – Gigacycle fatigue initiation mechanism in Armco iron, Int Jl Fatigue, Vol 45(2012)91-97
[8] C. Wang, A. Blanche, D. Wagner, A. Chrysochoos, C. Bathias – Study of Fatigue Crack initiation mechanism on an Armco Iron by dissipation assessments and microstructural observations, Crack Path 2012, Gaeta, Italie, septembre 2012
[9] Z. Huang, D. Wagner, C. Bathias – Effect of carburizing treatment on the “fish eye” crack growth for a low alloyed chromium steel in Very High Cycle Fatigue, Mat. Sc.& Eng.A, article sous presse
[10] Z. Huang, D. Wagner, C. Bathias, P. C. Paris - Subsurface Crack Initiation and Propagation Mechanism in the Gigacycle Fatigue, Acta Materiala, 58 (2010), 6046-6054
[11] Y. Hong, Z. Lei, C. Sun, A. Zhao – Characteristics of crack interior initiation and early growth originated from inclusion for very high cycle fatigue of high strength steels, Crack Path 2012, Gaeta, Italie, septembre 2012